Tissue-Specific Consequences of Cyclin D1 Overexpression in Prostate Cancer Progression

Yue He,[1] Omar E. Franco,[2] Ming Jiang,[2] Karin Williams,[2] Harold D. Love,[2] Ilsa M. Coleman,[4] Peter S. Nelson,[4] and Simon W. Hayward[1,2,3]

Departments of [1]Cancer Biology and [2]Urologic Surgery, [3]Vanderbilt-Ingram Cancer Center, Vanderbilt University Medical Center, Nashville, Tennessee and [4]Divisions of Human Biology and Clinical Research, Fred Hutchinson Cancer Research Center, Seattle, Washington

Abstract

The cyclin D1 oncogene encodes the regulatory subunit of a holoenzyme that phosphorylates and inactivates the Rb protein and promotes progression through G_1 to S phase of the cell cycle. Several prostate cancer cell lines and a subset of primary prostate cancer samples have increased cyclin D1 protein expression. However, the relationship between cyclin D1 expression and prostate tumor progression has yet to be clearly characterized. This study examined the effects of manipulating cyclin D1 expression in either human prostatic epithelial or stromal cells using a tissue recombination model. The data showed that overexpression of cyclin D1 in the initiated BPH-1 cell line increased cell proliferation rate but did not elicit tumorigenicity *in vivo*. However, overexpression of cyclin D1 in normal prostate fibroblasts (NPF) that were subsequently recombined with BPH-1 did induce malignant transformation of the epithelial cells. The present study also showed that recombination of BPH-1 + cyclin D1–overexpressing fibroblasts ($NPF^{cyclin\ D1}$) resulted in permanent malignant transformation of epithelial cells ($BPH\text{-}1^{NPF\text{-}cyclin\ D1}$ cells) similar to that seen with carcinoma-associated fibroblasts (CAF). Microarray analysis showed that the expression profiles between CAFs and $NPF^{cyclin\ D1}$ cells were highly concordant including cyclin D1 up-regulation. These data indicated that the tumor-promoting activity of cyclin D1 may be tissue specific. [Cancer Res 2007;67(17):8188–97]

Introduction

Prostate development is controlled by steroid hormones that induce and maintain a complex cross-talk between the stromal and epithelial cells (1). The result of this intercellular communication depends on the context and differentiation status of the cell type being stimulated (2, 3). The process of prostatic carcinogenesis includes aberrations in the interactions of the prostatic epithelium and its local microenvironment resulting in reciprocal dedifferentiation of both the emerging carcinoma cells and the prostatic smooth muscle.

The vast majority of human prostatic cancers arise as adenocarcinomas, which, by definition, are derived from the epithelial cells that form the glands and ducts of the prostate. As the carcinoma evolves, phenotypic changes and alterations in gene expression also occur in the adjacent stroma. These "changes" may enhance the invasive potential of the epithelial tumor (4–6). Chung et al. (7) reported that coinoculation of tumorigenic Nbf-1 fibroblasts with human PC-3 cells accelerated tumor growth. Human prostatic carcinoma-associated fibroblasts (CAF) have also been shown to be capable of stimulating carcinogenesis and inducing the progression of an initiated epithelium (the SV40 immortalized BPH-1 cell line), whereas normal prostate fibroblasts (NPF) were incapable of stimulating such progression (8). The mechanistic basis by which stromal-epithelial interactions enhance the process of prostatic carcinogenesis and tumor invasion is beginning to be dissected (6, 9).

The cells in the tumor microenvironment supporting and nurturing the developing tumor include stromal fibroblasts, infiltrating immune cells, blood, and lymphatic vascular networks (10). A detailed understanding of the changes occurring within tumor stroma and to the signaling mechanisms acting between stroma and epithelium will allow for the rational design of therapies aimed at inhibiting prostate tumor growth.

Cyclin D1 encodes the regulatory subunit of a holoenzyme that phosphorylates and inactivates the retinoblastoma protein and promotes progression through G_1 to S phase of the cell cycle (11, 12). Overexpression of cyclin D1 plays important roles in the development of human cancers, including breast, colon, and melanoma (11, 13–17). Increased cyclin D1 expression occurs relatively early during tumorigenesis; however, its role in prostate cancer is not well understood. Studies have shown that mouse prostatic normal and $Rb^{-/-}$ epithelial cells have elevated cyclin D1 expression as they enter the cell cycle (18). Human prostate carcinoma cell lines frequently express elevated levels of cyclin D1 protein, although the gene is not amplified in these cells (18). This situation is analogous to that seen in a subset of human breast cancer cell lines and tumors (19, 20). Overexpression of cyclin D1 can increase tumorigenicity of LNCaP cell lines. Additionally, androgen ablation has a smaller inhibitory effect on tumors formed by cyclin D1–overexpressing LNCaP cells compared with tumors formed by parental LNCaP cells, which regress after castration. This phenomenon suggests that cyclin D1 overexpression might be related to the evolution of androgen-independent prostate cancer (21). Immunostaining studies indicated that primary prostate carcinoma samples displayed moderate or strong expression of cyclin D1 protein in the epithelial compartment compared with normal epithelium. Little is known about the role of cyclin D1 in the stromal compartment of tumors, especially in adenocarcinomas. One study of cyclin D1 expression in esophageal carcinomas indicated that cyclin D1 is strongly expressed in stromal fibroblasts (22).

In this study, we examined the consequences of targeted regulation of cyclin D1 expression in epithelial or stromal cells to investigate the effects of cyclin D1 in prostate cancer progression.

Note: Supplementary data for this article are available at Cancer Research Online (http://cancerres.aacrjournals.org/).

Requests for reprints: Simon W. Hayward, Department of Urologic Surgery, Vanderbilt University Medical Center, A1302 MCN, Nashville, TN 37232-2765. Phone: 615-322-5823; Fax: 615-322-8990; E-mail: simon.hayward@vanderbilt.edu.

doi:10.1158/0008-5472.CAN-07-0418

Materials and Methods

Cells. BPH-1 (a nontumorigenic prostate epithelial cell) and its tumorigenic derivatives BPH^{CAFTD1} and BPH^{CAFTD2} were from our own stocks (23, 24). DU145, LNCaP, and PC-3 cells were obtained from American Type Culture Collection (ATCC). NPF, BPH fibroblasts, and CAFs were isolated and bioassayed as described previously (8). Prostatic epithelial cell (PrE) 1 cells were isolated from human benign prostate tissue. 957E/hTERT cells were generously supplied by Dr. John Isaacs (Johns Hopkins Oncology Center, Baltimore, MD). PrE3 cells were kindly provided by Dr. Dean Tang (The University of Texas M. D. Anderson Cancer Center, Houston, TX). BPH-1$^{C7\text{-}cyclin\ D1}$, BPH-1$^{C7\text{-}\Delta}$, BPH-1^{NPF}, NPF$^{cyclin\ D1}$, and BPH-1$^{NPF\text{-}cyclin\ D1}$ cells were generated as described below. All of the epithelial cells were maintained in RPMI 1640 (Life Technologies) with 1% antibiotic/antimycotic (Life Technologies) and 5% cosmic calf serum (CCS; HyClone). All of the stromal cells were maintained in the same condition except that 5% fetal bovine serum (Atlanta Biologicals) was used in place of CCS.

Construction of cyclin D1 expression vector. The plasmid C7-cyclin D1 was constructed using the LZRS-EGFP backbone (Nolan Laboratory, Stanford University, CA). The cytomegalovirus promoter was cut from pIRES-EGFP (Clontech) as a *Bgl*II/*Bam*HI fragment. The fragment was then ligated into the *Bam*HI site of the LZRS-EGFP backbone to produce C7-Δ. The human cyclin D1 cDNA clone was obtained from ATCC and amplified by PCR using a 5′ primer specific to translational start site and a 3′ primer containing an *Xho*I restriction site and the consensus sequence for the translational stop site. After PCR amplification, the product was gel purified and cloned into pGemT-Easy (Promega). Following DNA sequence verification, the cyclin D1 coding region was cut using *Eco*RI/*Xho*I and subcloned into the *Eco*RI/*Xho*I sites of pLZRS-EGFP to obtain C7-cyclin D1 construct.

Generation of a stable cyclin D1–overexpressing BPH-1 cell line. Viral particles were prepared as described previously and used to infect BPH-1 cells (25). Fresh virus was placed onto target cells every 24 h until green fluorescent protein (GFP) expression was observed. Cell sorting was done to select the GFP-expressing BPH-1 cells. Two stable cell lines were generated: C7-cyclin D1–overexpressing BPH-1 cell line and C7-Δ control BPH-1 cell line, which were designated as BPH-1$^{C7\text{-}cyclin\ D1}$ and BPH-1$^{C7\text{-}\Delta}$, respectively.

Generation of NPF$^{cyclin\ D1}$ cells. Human prostatic cells were prepared as described previously (25). Cyclin D1 virus was generated using phoenix A cells, and the prostatic cells were infected as described (25). After 1 week of successive rounds of infection, some cells expressed enhanced GFP (EGFP) when monitored by fluorescence microscopy. Differential trypsinization was used to separate fibroblasts from the epithelial cells. The resulting colonies were characterized by phenotype and their nature was confirmed using immunocytochemical staining against keratin and vimentin. After 12 passages, EGFP-expressing cells self-sorted as all unstained cells became senescent and died.

Western blotting analysis. Cell lysates were prepared and Western blotting was done as described previously (25). Membranes were incubated with mouse monoclonal antibody to cyclin D1 (1:1,000 dilution; BD Biosciences PharMingen) or α-tubulin (1:1,000 dilution; Santa Cruz Biotechnology) overnight, washed with PBS-Tween 20 for 1 h, and incubated with horseradish peroxidase (HRP)–linked antimouse or antirabbit secondary antibody (1:1,000 dilution; Amersham Biosciences) for 1 h. Bound antibodies were visualized using enhanced chemiluminescence Western blotting detection reagents (Amersham Bioscences). Cyclin D1 expression levels were normalized to β-actin and quantitated using Image J software from the NIH.[5]

Growth curves. BPH-1$^{C7\text{-}\Delta}$ and BPH-1$^{C7\text{-}cyclin\ D1}$ cells were plated in a 24-well plate (1,000 cells per well) in RPMI 1640 supplemented with 5% CCS. After the cells had attached overnight, 300 μL of CellTiter 96 Aqueous One Solution (Promega) were added at indicated times (1–5 days) to each well and the absorbance was measured at 490 nm after 3 h of incubation at 37°C. Experiments were done in triplicate.

Wound healing assays. Confluent monolayers of BPH-1$^{C7\text{-}\Delta}$ and BPH-1$^{C7\text{-}cyclin\ D1}$ cells were grown in six-well plates. An even line of cells was displaced by scratching through the layer using a pipette tip. Specific points on the wounds were identified and marked. These open areas were then inspected microscopically over time as the cells move in and fill the damaged area. Wounds were imaged at 0, 3, 6, and 8 h postwounding and the cell migration rate into the wound was calculated. Experiments were done in triplicate.

Transwell migration assay. One hundred thousand BPH-1$^{C7\text{-}\Delta}$ or BPH-1$^{C7\text{-}cyclin\ D1}$ cells were plated on top of the 8-μm pore polycarbonate culture inserts (Becton Dickinson Labware), which were situated in wells of a 24-well culture plate and immersed in RPMI 1640 supplemented with 5% CCS. The cells were incubated at 37°C for 12 h. The cells on the upper surface of the inserts were removed using cotton swabs and those that had migrated to the bottom side were fixed with 11% glutaraldehyde (Sigma) for 20 min and stained with 0.1% crystal violet (Sigma) for 20 min. Inserts were then washed with water three times. The number of cells that had migrated was counted using a microscope. The filters were viewed under bright-field optics to count stained cells in eight fields (with a 20× objective) for the two types of cells. The mean number of cells per field was determined, and results from at least three experiments were expressed as the mean relative cell migration ± SD, with that of BPH-1$^{C7\text{-}\Delta}$ cells set at 1.

Boyden chamber assay. Polycarbonate culture inserts with 8-μm pores were coated with 20 μL of 2.5 mg/mL Matrigel (BD Biosciences). After the gel solidified, the chambers were equilibrated with RPMI 1640 with 5% CCS for 2 h in a humidified tissue culture incubator at 37°C with 5% CO_2 atmosphere. More media were then added to the lower compartment, and 100k BPH-1$^{C7\text{-}\Delta}$ and BPH-1$^{C7\text{-}cyclin\ D1}$ cells were seeded in the upper compartment of the chamber. Each cell group was plated in three duplicate wells. After 12 h of incubation, the Matrigel was removed using a cotton swab. The number of cells that had migrated to the lower sides of the membrane was then determined as described for the Transwell migration assay.

Tissue recombination and xenografting. One hundred thousand epithelial cells and 300k stromal cells were recombined to make the BPH-1$^{C7\text{-}\Delta}$ + rat urogenital mesenchyme (rUGM), BPH-1$^{C7\text{-}cyclin\ D1}$ + rUGM, BPH-1 + NPF, and BPH-1 + NPF$^{cyclin\ D1}$ tissue recombinants as described previously (26). After incubating overnight at 37°C, the tissue recombinants were grafted under the kidney capsule of adult male severe combined immunodeficient (SCID) mice (Harlan). All the experiments were repeated six times. Mice were sacrificed after 4 weeks and grafts were harvested, fixed, and embedded.

Immunohistochemical staining. Immunohistochemical staining was done following a protocol that was described previously (25). Tissue slides were incubated with the primary antibody against SV40 (1:1,000 dilution; Santa Cruz Biotechnology), E-cadherin (1:1,000; BD Biosciences PharMingen), or anti–phospho-histone H3 (1:200; Upstate) overnight. The polyclonal rabbit or mouse immunoglobulins/biotinylated antimouse secondary antibody (DAKO) was incubated for 60 min after the slides were washed with PBS buffer for 1 h. After washing the slides in PBS extensively, slides were incubated in ABC-HRP complex (Vector Laboratories) for 30 min. Bound antibodies were then visualized by incubation with liquid 3,3′-diaminobenzidine tetrahydrochloride (DAKO). Slides were then rinsed extensively in tap water, counterstained with hematoxylin, and mounted.

Isolation of cell strains and regrafting. BPH-1^{NPF} and BPH-1$^{NPF\text{-}cyclin\ D1}$ cells were isolated and selected with 50 μg/mL G418 (Clontech) from BPH-1 + NPF and BPH-1 + NPF$^{cyclin\ D1}$ grafts and regrafted without stromal cells to SCID mice as described previously (27). Four to 14 weeks after grafting, the hosts were sacrificed. The harvested grafts were removed from the kidney and formalin fixed for immunohistochemical analysis.

Cell cycle analysis. BPH-1^{NPF} cells and BPH-1$^{NPF\text{-}cyclin\ D1}$ cells were harvested from monolayer culture. The cell pellets were washed, counted, and resuspended in PBS and fixed with 80% ethanol with vortexing. Cells were then pelleted and resuspended with PBS containing 1% CCS for cell counting after storing at −20°C for 4 h. One hundred thousand cells were

[5] http://rsb.info.nih.gov/ij/

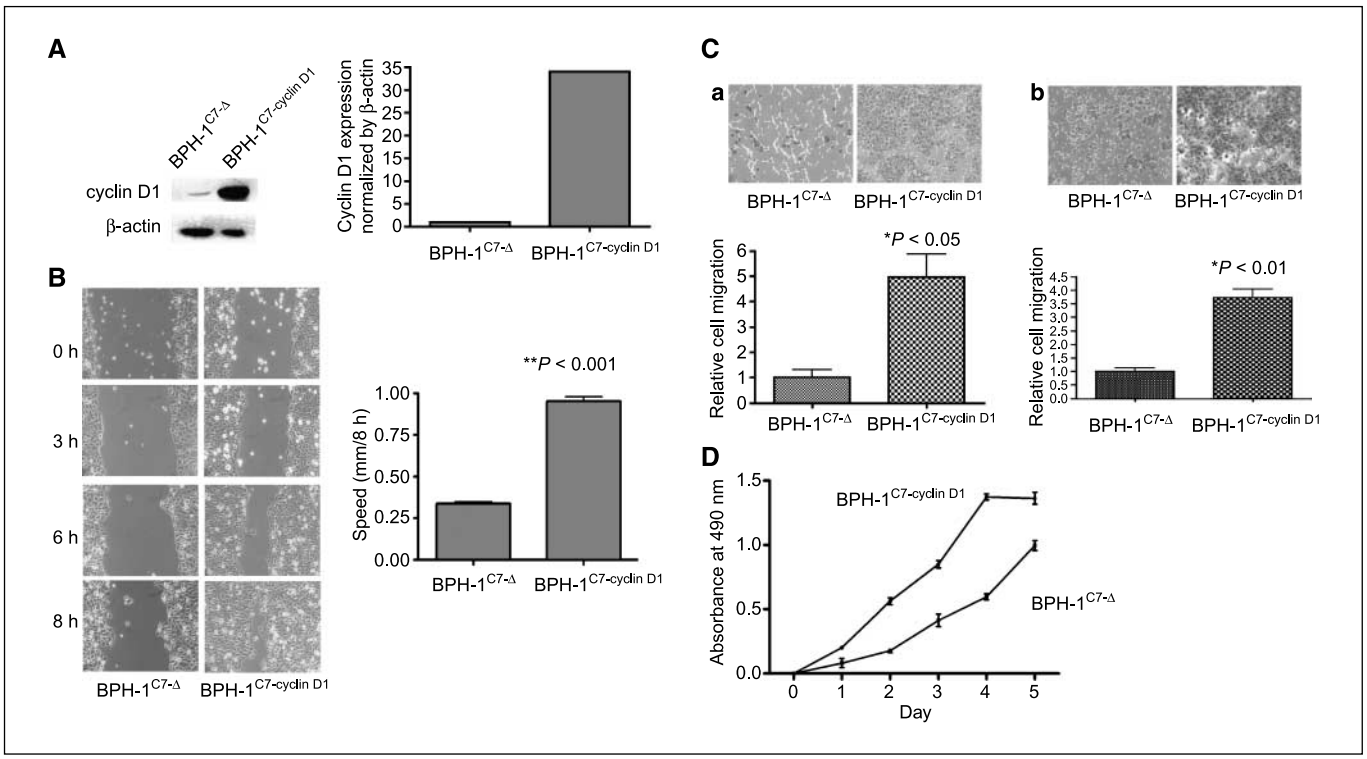

Figure 1. *In vitro* comparison of BPH-1$^{C7\text{-}\Delta}$ and BPH-1$^{C7\text{-cyclin D1}}$ cells. *A,* to examine the role of cyclin D1 in prostate cancer progression, C7-Δ (control – BPH-1$^{C7\text{-}\Delta}$) and cyclin D1–overexpressing (BPH-1$^{C7\text{-cyclin D1}}$) BPH-1 cell lines were generated by stable retroviral infection. Cyclin D1 overexpression in BPH-1$^{C7\text{-cyclin D1}}$ was confirmed by Western blotting and band intensity was quantitated. *B,* wound healing assay. BPH-1$^{C7\text{-cyclin D1}}$ closed wounds in the confluent monolayer were significantly faster than BPH-1$^{C7\text{-}\Delta}$ cells. Images (*left*) and quantitation (*right*). $P < 0.001$, Student's t test. *C,* Transwell migration study and invasion assay. BPH-1$^{C7\text{-cyclin D1}}$ migrated through the uncoated Boyden chamber significantly faster than BPH-1$^{C7\text{-}\Delta}$. Representative phase-contrast optical photomicrographs after overnight culture were shown (*a, top*) and quantitated (*a, bottom*). $P < 0.05$, Student's t test. BPH-1$^{C7\text{-cyclin D1}}$ cells had increased invasive ability in a Matrigel-coated Boyden chamber invasion assay compared with BPH-1$^{C7\text{-}\Delta}$. Representative phase-contrast optical photomicrographs after overnight culture were shown (*b, top*) and quantitated (*b, bottom*). $P < 0.01$, Student's t test. *D,* proliferation assay. Cyclin D1 overexpression promoted BPH-1 cell proliferation significantly over control growth rate. $P < 0.001$, Student's t test.

resuspended in propidium iodide/RNase/1% CCS/PBS. Propidium iodide was used to stain double-stranded nucleic acids stoichiometrically. Cells were treated with RNase A to stain only the DNA. Cell cycle distribution was analyzed on the flow cytometer after at least 30 min.

Microarray analysis. NPF$^{cyclin\ D1}$ cells were generated from NPFs, which were isolated from two different patient samples; CAFs were isolated from two different patient samples as well. RNA was isolated from NPFs, CAFs, and NPF$^{cyclin\ D1}$ cells using total RNA isolation kit (Qiagen). Custom spotted cDNA microarrays were constructed as described previously (28) using a nonredundant set of 6,700 prostate-derived cDNA clones identified from the prostate expression data base, a public sequence repository of expressed sequence tag data derived from human prostate cDNA libraries. Total RNA was amplified through one round of linear amplification using the MessageAmp aRNA kit (Ambion). Sample quality and quantification was assessed by agarose gel electrophoresis and absorbance at A_{260}. Cy3-labeled and Cy5-labeled cDNA probes were made from 4 μg of amplified RNA. Two NPF$^{cyclin\ D1}$ and two CAF samples (labeled with Cy3) were hybridized head-to-head with a NPF control sample labeled with Cy5. Probes were hybridized competitively to microarrays under a coverslip for 16 h at 63°C. Fluorescent array images were collected for both Cy3 and Cy5 by using a GenePix 4000B fluorescent scanner, and image intensity data were gridded and extracted using GenePix Pro 4.1 software. Differences in gene expression between NPF$^{cyclin\ D1}$/NPF and CAF/NPF groups were determined using a two-sample t test with Significance Analysis of Microarrays (SAM) software[6] with a false discovery rate (FDR) of ≤10% considered significant (Tusher, 2001). Similarities in gene expression between NPF$^{cyclin\ D1}$/NPF and CAF/NPF groups were determined using a one-sample t test in SAM with a FDR of ≤0.1% considered significant. These results were reduced to unique genes by eliminating all but the highest scoring clones for each gene. A Pearson correlation coefficient was calculated in Excel to assess the strength of the linear relationship between NPF$^{cyclin\ D1}$/NPF and CAF/NPF average log 2 ratios.

[6] http://www-stat.stanford.edu/_tibs/SAM/

Results

Cyclin D1 expression levels are elevated in malignant human prostatic epithelial cell lines. Cyclin D1 expression was examined by Western blotting in the prostate cancer cell lines, DU145, LNCaP, BPH^{CAFTD1}, and BPH^{CAFTD2}, and in a subset of nontumorigenic prostatic cells, PrE1, 957E/hTERT (27, 29), PrE3, and BPH-1 cell line. Cyclin D1 expression was found to be higher in all of the cancer cells compared with the nontumorigenic prostatic cells. A representative Western blot is shown in Supplementary Fig. S1. Primary epithelial cells had the lowest cyclin D1 expression. The SV40 T-antigen immortalized BPH-1 cells had higher cyclin D1 expression compared with PrE, 957E/hTERT and PrE, but lower expression level than that in malignant cell lines. These data crudely correlate cyclin D1 with tumorigenicity but, as with similar correlations seen in patient samples, do not address whether cyclin D1 overexpression is a cause or an effect of malignant change. To address this question, we tested the consequences of overexpressing cyclin D1 in nontumorigenic prostatic epithelial cells.

Cyclin D1 overexpression in BPH-1 cells can increase cell proliferation rate, migration, and invasive ability *in vitro*. Western blotting showed that the BPH-1$^{cyclin\ D1}$ cells have a 34-fold elevation in cyclin D1 expression compared with control BPH-1$^{C7\text{-}\Delta}$ cells (Fig. 1*A*). BPH-1$^{C7\text{-cyclin D1}}$ cells showed enhanced motile ability in wound healing, Transwell migration, and Boyden chamber assays. Wound healing assays showed that BPH-1$^{C7\text{-cyclin D1}}$ cells were significantly more motile than BPH-1$^{C7\text{-}\Delta}$ cells. This difference was clear after 3 h and was very marked after 8 h ($P < 0.001$, Student's *t* test; Fig. 1*B*). In a Transwell migration study, the BPH-1$^{C7\text{-cyclin D1}}$ cells migrated through the uncoated Boyden chambers to the underside of the insert in greater numbers in a 12-h response to conditional medium containing 1% CCS in the lower chamber than BPH-1$^{C7\text{-}\Delta}$ cells ($P < 0.05$, Student's *t* test; Fig. 1*C*). These data confirmed the elevated motility of BPH-1$^{C7\text{-cycin D1}}$ cells, as seen in the wound healing assay. An invasion assay, in which the inside chamber was coated with Matrigel to mimic the *in vivo* extracellular matrix (ECM), showed that BPH-1$^{C7\text{-cyclin D1}}$ cells had significantly increased invasive activity *in vitro* ($P < 0.01$, Student's *t* test; Fig. 1*D*). We used a 3-(4,5-dimethylthiazol-2-yl)-2,5-diphenyltetrazolium bromide assay to assess the effect of cyclin D1 overexpression on the growth rate of BPH-1 cells. Our results showed that the cyclin D1–overexpressing cells proliferated faster than control cells. The difference was observed even after 24 h of incubation (Fig. 1*E*). Collectively, the assays showed that when cyclin D1 is forcibly overexpressed, BPH-1 cells acquired an enhanced proliferation rate, motility, and invasive ability *in vitro*.

Cyclin D1–overexpressing BPH-1 cells are not tumorigenic in tissue recombinants with rUGM. To determine whether cyclin D1 could exert a tumorigenic effect on prostate cells *in vivo*, 100k BPH-1$^{C7\text{-cyclin D1}}$ cells or control cells were recombined with 300k rUGM and grafted under the kidney capsule of SCID mice. The grafts were harvested after 4, 8, 12, and 16 weeks. The results showed that BPH-1$^{C7\text{-cyclin D1}}$ cells formed significantly larger and

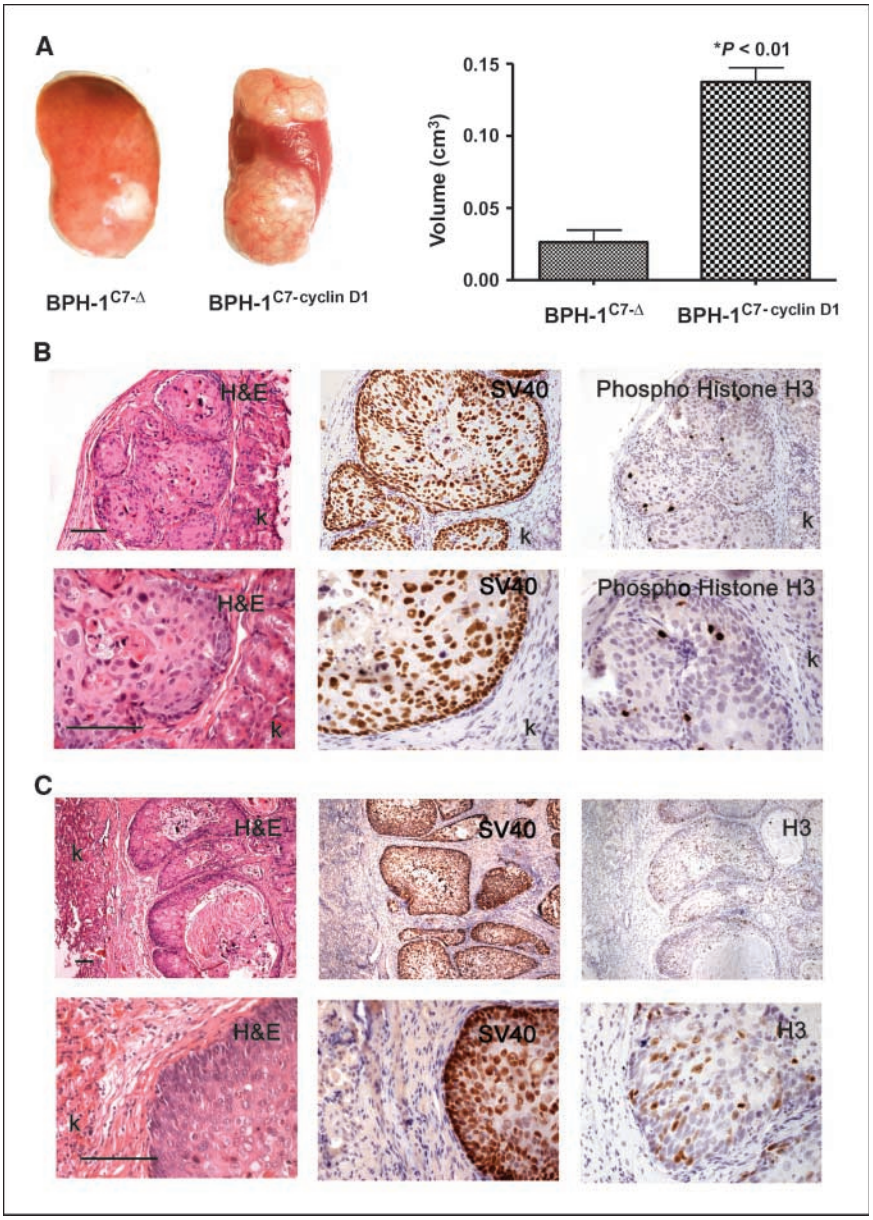

Figure 2. Overexpression of cyclin D1 in epithelium was insufficient to induce malignant transformation in BPH-1 cells as determined by *in vivo* assays. *A,* BPH-1$^{C7\text{-cyclin D1}}$ cells were not tumorigenic under the influence of the inductive rUGM in the tissue recombination model. Gross morphology of 2-month grafts of BPH-1$^{C7\text{-}\Delta}$ + UGM (*left*) and BPH-1$^{C7\text{-cyclin D1}}$ + UGM (*right*). The volume of grafts containing BPH-1$^{C7\text{-cyclin D1}}$ was significantly larger than controls. $P < 0.01$, Student's *t* test. *B,* H&E staining of BPH-1$^{C7\text{-}\Delta}$ + UGM grafts showed that the recombinants formed solid cord structures with no sign of invasion to the host kidney. SV40 T-antigen staining confirmed the cell origin of the epithelium. Phospho-histone H3 staining identified few positive cells in the solid cords. Higher magnification pictures (*bottom*). *Bar*, 50 μm. *C,* H&E and SV40 T-antigen staining of BPH-1$^{C7\text{-cyclin D1}}$ + UGM grafts. Histology is similar to that seen in the control groups. The basement membrane between kidney and graft was intact and no sign of invasion into the host kidney was seen. Phospho-histone H3 staining identified significantly more positive cells in the solid cords compared in (*B*). Higher-magnification images (*bottom*). *Bar*, 50 μm. *k,* host kidney.

more vascularized grafts under the induction of rUGM compared with BPH-1$^{C7\text{-}\Delta}$ cells. An example of the gross morphology of grafts at 8 weeks is shown in Fig. 2*A*. These results are consistent with our *in vitro* experiments, which showed that BPH-1$^{C7\text{-cyclin D1}}$ cells proliferate faster than controls. Histologically, both experimental and control grafts exhibited the formation of solid epithelial cords surrounded by a muscular stroma. SV40 T-antigen staining confirmed the origin of BPH-1 cells in both control and cyclin D1–overexpressing groups and showed that there were sharp delineations from the host kidney with no sign of invasion (Fig. 2*B* and *C*). It was noteworthy that a clear layer of stromal cells was always seen between the graft and host kidney under both control and test conditions. In the control grafts, few epithelial cells were phospho-histone H3 positive (indicating low proliferation rates). However, there were significantly more histone H3–positive cells in BPH-1$^{\text{cyclin D1}}$ cords ($P < 0.01$, Student's t test; data not shown). These data indicated that BPH-1$^{\text{cyclin D1}}$ cells proliferated much faster than control cells (Fig. 2*B* and *C*). To assess whether cyclin D1 can transform BPH-1 cells in a longer period *in vivo*, we sacrificed mice every month for up to 4 months. The histologic appearance of the grafts at 4 months was similar to the earlier grafts with solid cord structures and no invasion of the kidney (date not shown). Therefore, although cyclin D1 can increase BPH-1 cell motility and promote cell proliferation *in vitro*, overexpression of the gene did not induce BPH-1 cells to undergo malignant transformation with associated invasion.

NPF$^{\text{cyclin D1}}$ cells have increased life span compared with NPFs and CAF cells have up-regulated cyclin D1 expression. Because the stroma is viewed as an important active contributor to tumor growth and to understand whether cyclin D1 does different functions in stromal and epithelial tissues, we generated NPF$^{\text{cyclin D1}}$ cells by overexpressing cyclin D1 in primary cultures of normal prostate stromal cells. To investigate whether the cyclin D1–overexpressing fibroblasts have an increased life span compared with control or noninfected cells, we passaged the cell mixtures 12 times. The uninfected cells underwent spontaneous senescence and died within 12 passages. The EGFP-expressing cells still looked healthy and grew well after 11 more passages (total of 23 passages; Fig. 3*A*). Western blot analysis showed that EGFP-positive cells also overexpressed cyclin D1 (Fig. 3*B*). This result indicated that NPFs acquired a prolonged life span as a consequence of up-regulated cyclin D1.

It has been shown previously that CAF cells can induce BPH-1 cells to undergo malignant transformation, whereas NPFs cannot (8). Cyclin D1 is strongly expressed in stromal fibroblasts in carcinoma and adenocarcinoma (22). We were interested to determine whether human prostatic CAFs have elevated cyclin D1 expression and if so whether CAFs and NPF$^{\text{cyclin D1}}$ cells share common functional sequelae. Therefore, we examined the expression level of cyclin D1 in NPFs, BPH fibroblasts, and CAF cells. These experiments showed that CAFs expressed a much higher level of cyclin D1 protein than either NPFs or fibroblasts isolated from BPH patients (Fig. 3*B*).

NPF$^{\text{cyclin D1}}$ cells elicit CAF-like effects promoting tumorigenesis. To investigate the *in vivo* consequences of overexpression of cyclin D1 in NPFs, 100k BPH-1 cells were recombined with either 300k NPF$^{\text{cyclin D1}}$ or NPF cells. Grafts were harvested after 1 month. Tissue recombinants composed of BPH-1 + NPF$^{\text{cyclin D1}}$ exhibited moderate growth; in contrast, consistent with previously published data, control recombinants composed of BPH-1 + NPFs showed minimal growth. Control grafts of NPF and NPF$^{\text{cyclin D1}}$ were likewise

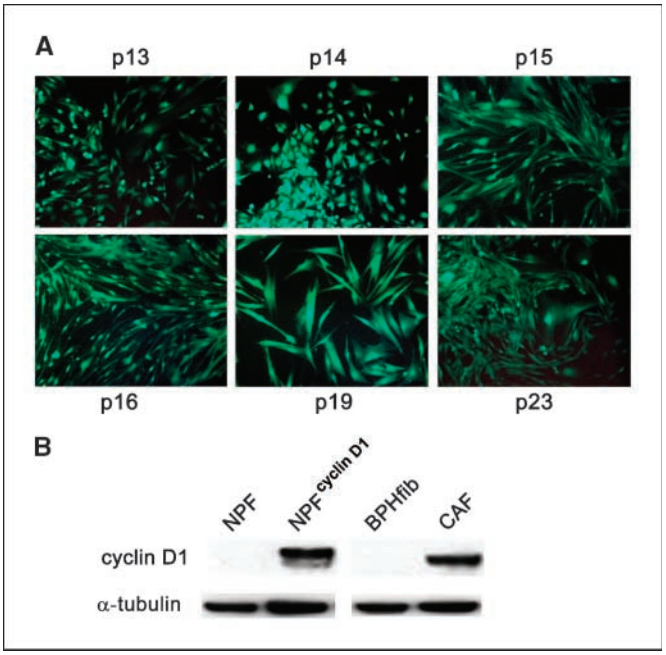

Figure 3. Expression of cyclin D1 in human prostatic fibroblasts. *A,* NPF$^{\text{cyclin D1}}$ cells have increased life span compared with NPF cells. Control cells were all dead within 12 passages. The NPF$^{\text{cyclin D1}}$ cells seemed healthy after 23 passages (passage number shown adjacent to illustration) after infection by C7-cyclin D1–overexpressing retroviral vector (total of 23 passages). *B,* Western blotting results confirmed that cyclin D1 was overexpressed in NPF$^{\text{cyclin D1}}$ cells. Human prostatic CAF cells also expressed elevated levels of cyclin D1 protein compared with NPF or with BPH-derived fibroblasts.

small and flattened (Fig. 4*A, a* and *b*). Comparison between the volume of the control and test recombinants showed that the test samples were significantly larger ($P < 0.01$, Student's t test). The histologic appearance of the BPH-1 + NPF$^{\text{C7-cyclin D1}}$ grafts, as assessed by H&E staining, resembled a poorly differentiated carcinoma with areas of squamous differentiation (Fig. 4*B, a* and *b*). Instead of forming solid cord structures, some epithelium fused to form large nests with keratinization and a broad pushing margin against the host kidney (Fig. 4*B, a* and *b*). Tumors also contained irregular epithelial cords intermingled within a fibrous stroma [Fig. 4*B, e* and *f* (*right arrow*)]. In other areas, single epithelial cells were intermixed with fibrous stroma [Fig. 4*B, c* (*arrow*) and *f* (*left arrow*)]. SV40 T-antigen staining confirmed the origin of the epithelial component of the tumors as being from the BPH-1 cells (Fig. 4*B, c* and *f*). E-cadherin expression was patchy, with positive expression in cell-cell junctions in some areas but weak or absent in many areas (Fig. 4*B, d*). The histology of recombinants of BPH-1 + NPF$^{\text{cyclin D1}}$ was similar to that previously described for BPH-1 + CAF recombinants (8, 30), although the overall tumor size was smaller. After 5 months of incubation in the kidney capsule, BPH-1 cells formed larger tumors with clear kidney invasion (Fig. 4*B, g* and *i*). Small kidney tubes intermingled with tumor cells [Fig. 4*B, g* (*arrows*) and *h* (*arrow*)] and there were no clear margins between the kidney and grafts.

In contrast to the malignant histologic appearance of the BPH-1 + NPF$^{\text{cyclin D1}}$ recombinants, the BPH-1 + NPF recombinants appeared benign and, as described previously, the bulk of the grafts were composed of stromal cells. Occasional small epithelial cords were found (Fig. 4*B, k* and *l*). This confirmed previous observations that stromal cells from normal peripheral zone recombined with BPH-1 cells produced benign or no visible grafts (8, 30).

To examine if NPF$^{\text{cyclin D1}}$ cells are tumorigenic, we grafted either NPF or NPF$^{\text{cyclin D1}}$ cells alone to SCID mice. Both control groups formed flattened grafts (Fig. 4*A, c* and *d, arrows*). H&E staining showed that both grafts were present as a thin layer of fibrous tissue (data not shown).

Epithelial cells isolated from BPH-1 + NPF$^{\text{cyclin D1}}$ grafts (BPH-1$^{\text{NPF-cyclin D1}}$) are tumorigenic. After cell culture and G418 selection, two cell strains were derived from BPH-1 + NPF and BPH-1 + NPF$^{\text{cyclin D1}}$ grafts, designated BPH-1$^{\text{NPF}}$ and BPH-1$^{\text{NPF-cyclin D1}}$. The two strains were grafted in collagen gels beneath the renal capsule of male SCID mice. Grossly, after 3 months, the BPH-1$^{\text{NPF-cyclin D1}}$ cells formed significantly larger grafts than the control group (Fig. 5*A, right*). The control group formed small flattened grafts (Fig. 5*A, left*). Histologically, the BPH-1$^{\text{NPF}}$ cells grew to form occasional small cords, which were SV40 positive, similar to the grafts reported previously for BPH-1 cells grafted alone (Fig. 5*B*). The BPH-1$^{\text{NPF-cyclin D1}}$ cells, in contrast, formed large fused nests generally with a broad pushing margin to the host kidney (Fig. 5*C, a, arrow*). Many smaller nests with irregular shapes were scattered throughout the tumor and intermingled with

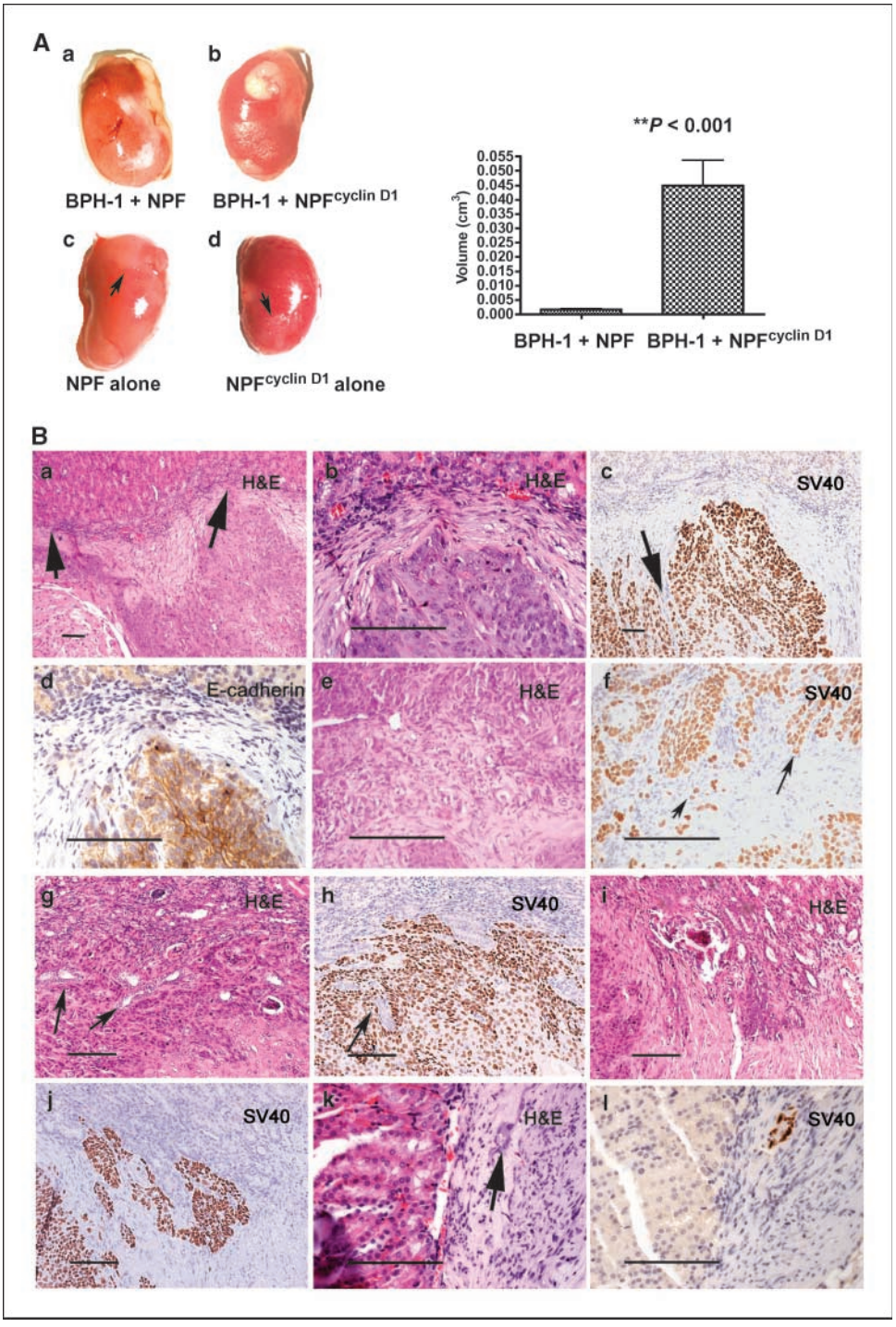

Figure 4. Effects of NPF$^{\text{cyclin D1}}$ cells on BPH-1 epithelium *in vivo*. *A,* gross morphology of 1-month grafts of tissue recombinants composed of BPH-1 + NPF (*a*), BPH-1 + NPF$^{\text{cyclin D1}}$ cells (*b*), NPF alone (*c*), and NPF$^{\text{cyclin D1}}$ alone (*d*). The graft volume of BPH-1 + NPF$^{\text{cyclin D1}}$ was significantly larger than that of BPH-1 + NPF. $P < 0.001$, Student's *t* test (*right*). *B,* staining of BPH-1 + NPF$^{\text{cyclin D1}}$ recombinants revealed organization resembling a poorly differentiated carcinoma. Some epithelium fused to form large nests (*a* and *b*) with keratinization and a broad pushing margin to kidney (*a, arrow*). Tumors contained irregular epithelial cords and epithelial cells intermingled within a fibrous stroma [*c, e*, and *f* (*right arrow*)]. Single epithelial cells were intermixed with fibrous stroma in other areas [*c* (*arrow*) and *f* (*left arrow*)]. Immunohistochemical localization of SV40 T antigen confirmed the origin of the tumors (*c* and *f*). E-cadherin staining was patchy (*d*). After 5 mo of incubation in kidney capsule, BPH-1 cells formed larger tumors and invaded the host kidney (*g–j*). Tumor cells surrounded and intermingled with kidney tubes [*g* and *h* (*arrow*)]. There were no clear margins between kidney and grafts. H&E staining of BPH-1 + NPF grafts revealed small grafts with minimal epithelial growth consistent with previous observations [*k* (*arrow*) and *l*]. *Bar*, 50 μm.

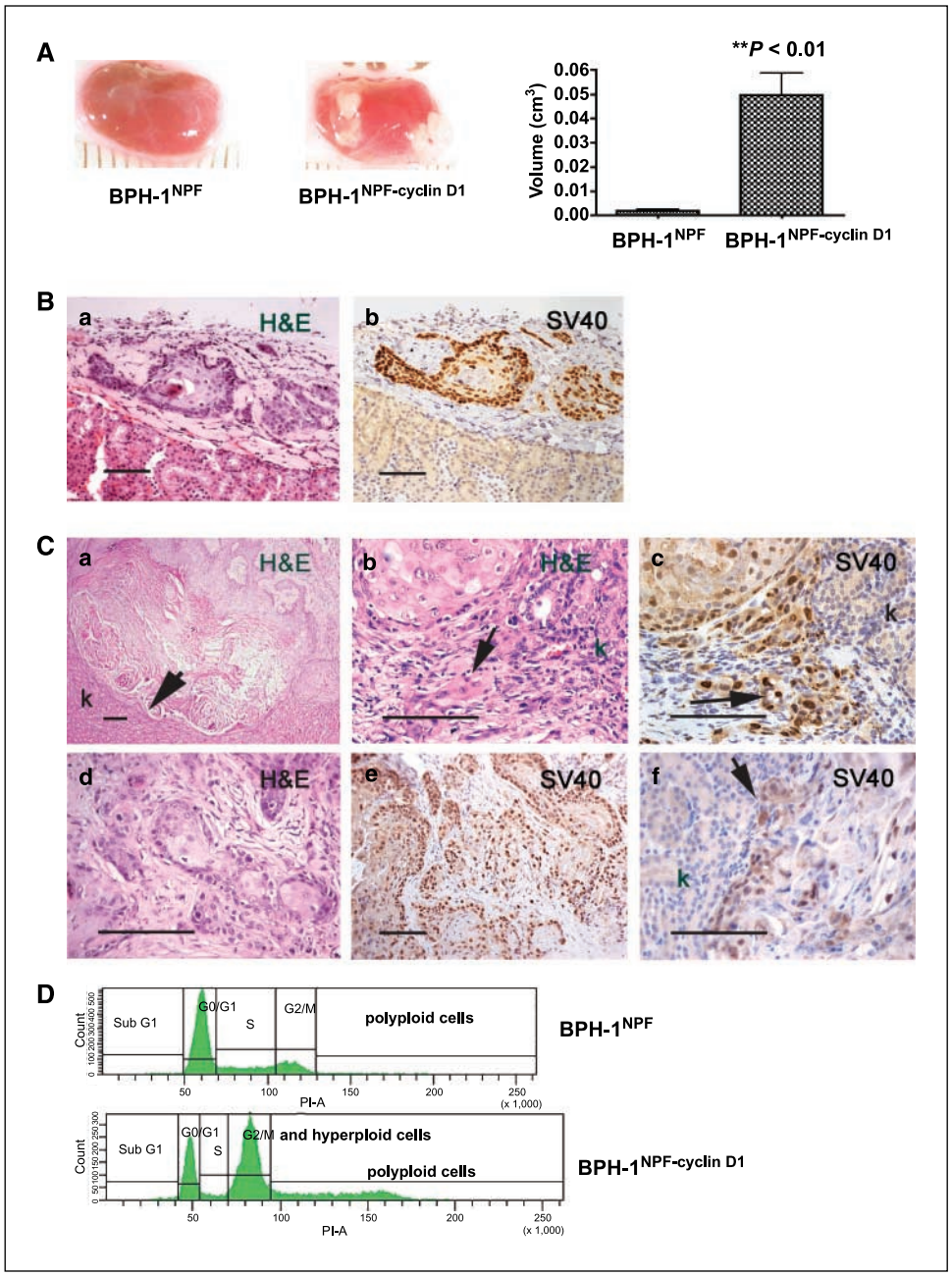

Figure 5. The BPH-1$^{\text{NPF-cyclin D1}}$ cells, which were isolated from BPH-1 + NPF$^{\text{cyclin D1}}$ grafts, exhibited a transformed phenotype. *A,* gross morphology of 3-month grafts of BPH-1$^{\text{NPF}}$ (*left*) and BPH-1$^{\text{NPF-cyclin D1}}$ (*right*). The volume of the BPH-1$^{\text{NPF-cyclin D1}}$ grafts was significantly larger than the control grafts. $P < 0.01$, Student's t test. *B,* in grafts of BPH-1$^{\text{NPF}}$ cells, occasionally, epithelial cords were seen (*a*) and their origin was confirmed by SV40 staining (*b*). No evidence of malignant growth or invasion was seen in these grafts. *Bar*, 50 μm. *C,* BPH-1$^{\text{NPF-cyclin D1}}$ tumors were larger than controls with areas of keratinization (*a*). The grafts formed a pushing margin directly touching the host kidney (*a, arrow*). Small nests of epithelial cells with irregular shapes intermingled with stroma (*d* and *e*). Some infiltrative areas (*b, arrow*) were found to be composed of bubbly cytoplasm and indistinct cells borders (*c, arrow*). Minimally invasive growth into the kidney was seen in a few areas. The invading cells expressed SV40 T antigen (*f, arrow*). *Bar*, 50 μm. *D,* fluorescence-activated cell sorting analysis showed striking differences in cell population distribution between BPH-1$^{\text{NPF}}$ and BPH-1$^{\text{NPF-cyclin D1}}$ cells. The majority (64%) of the BPH-1$^{\text{NPF}}$ cells were in the G_1-G_0 phase of cell cycle. In contrast, in BPH-1$^{\text{NPF-cyclin D1}}$ cells, an abnormal peak that contains 55% of the total cell population is located close to but somewhat below where the G_2-M peak would be expected. Additionally, polyploid cells are composed of 23.1% of the total population in the BPH-1$^{\text{NPF-cyclin D1}}$ cells.

stroma (Fig. 5*C, d* and *e*). Some infiltrative areas recapitulated prostatic carcinoma (Fig. 5*C, b, arrow*). Cells contained a foamy cytoplasm and their borders were indistinct (Fig. 5*C, c, arrow*). Minimally invasive growth was found in some areas (Fig. 5*C, f*). Tumors continued to express SV40 T-antigen confirming the BPH-1 origin of the malignant epithelium.

DNA flow cytometry analysis showed that stromal cyclin D1 caused a shift of the cell cycle distribution of BPH-1$^{\text{NPF-cyclin D1}}$ cells. An abnormal wider peak that contains 55% of the cell population is located close to where the G_2-M peak (which has twice the normal copies of DNA) is supposed to be, but its position is below the G_2-M peak position. It was reported that a wide peak may represent two populations of cells with different quantities of DNA (31). Given that the original BPH-1 population has been described previously to have an abnormal chromosomal make up and further that this can be altered by exposure to cancer stroma, it is possible that BPH-1$^{\text{NPF-cyclin D1}}$ cells became hyperdiploid or nearly tetraploid, and the hyperdiploid cell population mixed with the tetraploid G_2-M population to produce this abnormal peak. A large proportion (23.1%) of BPH-1$^{\text{NPF-cyclin D1}}$ cells also appear to be polyploid with varying but high DNA content. In marked contrast, only 0.9% of BPH-1$^{\text{NPF}}$ cells were found to be polyploid and BPH-1$^{\text{NPF}}$ cells showed a normal distribution of cell populations with 64% cells in the G_1 phase of cell cycle. (Fig. 5*D*).

Gene expression profiles were highly concordant between CAFs and NPF$^{\text{cyclin D1}}$ cells. The gene expression patterns of NPFs, CAFs, and NPF$^{\text{cyclin D1}}$ cells were compared by cDNA microarray analysis (Gene Expression Omnibus submission GSE6936; National Center for Biotechnology Information tracking system 15248638). NPF$^{\text{cyclin D1}}$ cells and CAFs showed a high level of gene expression

correlations when compared with NPFs (Pearson $r = 0.65$ across all 5,652 clones returning data in all four samples.) A one-sample t test in SAM identified 118 unique genes up-regulated and 51 unique genes down-regulated ($q \leq 0.1\%$) commonly expressed between NPF$^{\text{cyclin D1}}$ cells and CAFs when compared with NPFs. (Supplementary Figs. S2 and S3). Relatively few significant differences in transcript abundance measurements between NPF$^{\text{cyclin D1}}$ cells and CAFs were identified: a two-sample t test in SAM identified 6 unique genes up-regulated and 20 unique genes down-regulated ($q \leq 10\%$) in CAFs when compared with cyclin D1–overexpressing fibroblasts (Supplementary Fig. S4).

Discussion

The concept of stroma as a contributor to, and potentially an initiator of, carcinogenesis have led to altered perceptions of the development and progression of epithelial malignancies. Histopathologic examination has shown clear differences in gene expression patterns between the reactive stroma of tumors and normal stroma; additionally, these differences have clinical prognostic value (32–34). The importance of stromal-epithelial interactions in tumorigenesis has been shown in many malignancies, including, carcinoma of the skin, colon, breast, and prostate (35–38). Not only stromal-epithelial interactions play an important role in normal development and adult growth quiescence of the prostate (39) but also changes in these interactions can promote a malignant progression of initiated epithelium and result in tumorigenesis (2, 4, 32, 40, 41).

There are cases in which addition of a single dominant-acting oncogene is sufficient to transform a nontumorigenic cell. For example, massive overexpression of c-*myc* converted normal prostatic epithelial cells to rapidly become an invasive prostate carcinoma cell (25), whereas lower levels of c-myc expression had similar but slower effects (42). Similarly loss of genes with tumor suppressor function can also contribute to malignancy (43). These observations emphasize the importance of genetic changes as key factors in malignancy. Alterations in the microenvironment adjacent to the epithelial cells can drive nontumorigenic cells to become malignant both *in vivo* and *in vitro* (8, 44, 45). Stromal factors can also elicit reversion of a malignant teratocarcinoma to a benign phenotype despite genetic changes within the epithelial cells (46–48). The growth and differentiation of epithelial cells from R3327 Dunning prostatic adenocarcinoma (DT) were modified when reassociated with normal stromal environment. The epithelial cells were induced to differentiate to tall columnar secretory epithelial cells and tumorigenesis was remarkably diminished (48, 49). Experiments in mice suggested that genetic inactivation of the stromal transforming growth factor-β receptor II resulted in the transformation of normal epithelial cells (50). Bissell's group showed that by manipulating ECM proteins, human breast cancer cells reverted to normal functional cells in culture and tumorigenicity was reduced dramatically in mice (51).

Cyclin D1 is an important oncogene in many human cancers, but its function in prostate cancer is not clear (21, 52–55). We show here that cyclin D1 is up-regulated in prostate cancer cell lines, indicating that it might be associated with prostate tumorigenicity. Overexpression of cyclin D1 can increase tumorigenicity of LNCaP cell lines (21). We have observed that BPH-1 cells, in which cyclin D1 was overexpressed, did not become tumorigenic under the influence of inductive rUGM in the tissue recombination model when grafted to SCID mice. However, the cyclin D1–overexpressing cells did have a higher proliferation rate *in vitro* and *in vivo* and motility *in vitro*. Such observations indicated that this single gene is not enough to transform BPH-1 cells even in the face of SV40 large T antigen, which is expressed in these cells. This underlines the important point that increased proliferation per se is insufficient for malignant transformation.

In marked contrast to the effects in epithelial cells, overexpression of cyclin D1 in primary cultures of benign human prostatic fibroblasts extended the life span and altered the behavior of the stromal cells, nonetheless falling short of directly inducing malignant transformation. Cyclin D1 induced these cells to behave in a manner similar to CAFs, imparting an ability to elicit malignant transformation in BPH-1 epithelial cells in a tissue recombination model. The cyclin D1–overexpressing fibroblasts have increased life span compared with NPFs. NPFs were all dead within 12 passages. However, the NPF$^{\text{cyclin D1}}$ cells seemed healthy after an additional 11 passages. NPFs overexpressing cyclin D1 may be selectively advantageous for the proliferation and survival characteristics often associated with oncogenesis compared with noninfected cells in the same mixture. However, it should be noted that, as when expressed in epithelial cells, expression of cyclin D1 did not result in transformation of the stromal cell population. As a result of *in vitro* adaptation, cells may pick up generic alterations such as the mRNA changes we have seen in microarray data. However, NPF$^{\text{cyclin D1}}$ cells are not fully immortal and are not tumorigenic by themselves. This is consistent with observations that CAFs are also not immortal and not tumorigenic per se but have the ability to transform adjacent BPH-1 cells.

By expressing cyclin D1 in stromal cells, we showed that benign stromal cell behavior can be modified to mimic that of cancer stromal cells. NPF$^{\text{cyclin D1}}$ cells have a potential to transform BPH-1 cells similar to that seen with CAFs although with a reduced intensity. Tissue architecture in recombinants showed irregular epithelial cords and epithelium infiltrating into the stroma. This observation indicated that the presence of altered stromal cells in proximity to an initiated epithelium has an important biological effect on prostatic carcinogenesis. Expression of this single oncogene in the stroma may mimic the effects of CAFs on epithelium by modifying the local microenvironment. Specifically altering the expression of growth factors and ECM proteinases results in expansion and malignant progression of the initiated epithelial cells.

BPH-1 cells form tumors after recombination with CAFs and epithelial cells derived from these tumors (BPH-1$^{\text{CAFTD}}$) are tumorigenic without the stimulation of stromal cells when regrafted to mice (23). The present study shows that the tumorigenic behavior of BPH-1$^{\text{NPF-cyclin D1}}$ cells (derived from recombination of BPH-1 + NPF$^{\text{cyclin D1}}$ cells) also resulted in a permanent malignant transformation of epithelial cells similar to that seen with CAF.

Cell cycle analyses of cells from malignant tissues have shown the presence of aneuploid cells as well as normal diploid cells (56). In the present study, an abnormal peak in cell cycle histogram of BPH-1$^{\text{NPF-cyclin D1}}$ likely represented hyperdiploid cells. Many of these cells had multiple nuclei. It has been shown that aneuploidy is the possible underlying mechanism and potential consequences in the pathogenesis of human lung cancer (57). Clinical progression of prostate cancer is also associated with formation of DNA aneuploidy (58). These data suggested that BPH-1$^{\text{NPF-cyclin D1}}$ cells might be transformed through chromosomal changes (aneuploidy).

The histologic appearance of BPH-1$^{\text{NPF-cyclin D1}}$ tumors was consistent with poorly differentiated carcinoma. It is important to

note that CAFs have elevated expression levels of cyclin D1 protein; therefore, many of their characteristics could be linked to the downstream consequences of this change. Microarray comparison of the NPF$^{\text{cyclin D1}}$ and CAFs versus NPF showed highly concordant gene expression profiles. The same 118 unique genes were up-regulated and 51 unique genes were down-regulated in NPF$^{\text{cyclin D1}}$ cells and CAFs when compared with NPFs. Relatively few significant differences in transcript abundance measurements between NPF$^{\text{cyclin D1}}$ cells and CAFs were identified. These data indicate that cyclin D1 expression in stroma can critically affect paracrine interactions with adjacent epithelial cells in a manner resembling CAFs.

In summary, the present study showed for the first time the importance of cyclin D1 as a potential regulator of paracrine interactions in prostate cancer progression. The cyclin D1–overexpressing fibroblasts have an increased life span and share many commonalities with CAFs making them a potentially useful research tool. Traditional therapy for all epithelial malignancies, including prostate cancer, has been targeted at the epithelial cells that progressively acquire genetic changes. The stroma may provide a more stable target at which to direct treatment because the gene expression profile differs from that seen in normal tissues. We should also bear in mind that the tumor stromal compartment is heterogeneous and that CAFs are a mixed population of fibroblastic cells. Juxtacrine signaling between fibroblastic cells of different types may contribute to changes in overall paracrine signaling, which boosts the growth of epithelial cells. Interactions with other stromal cell types, including inflammatory cells or nerve cells, also turn out to be of critical importance. A better understanding of these complex interactions within the stroma and between stroma and epithelium, and the manner in which these are influenced by gene expression in stromal cells will allow for the rational design of therapies aimed at inhibiting prostate tumor growth.

Acknowledgments

Received 2/5/2007; revised 5/3/2007; accepted 6/12/2007.

Grant support: The taxpayers of the United States via NIH and Department of Defense-Prostate Cancer Research Program (DOD-PCRP) grants CA96403 and U54CA126505-01 (S.W. Hayward) and PC041158 and U54CA126540-01 (P.S. Nelson) and DOD-PCRP predoctoral fellowship W81XWH-07-1-0139 (Y. He). The Vanderbilt University Medical Center Institutional Flow Cytometry Core was supported by the Vanderbilt Ingram Cancer Center grant P30CA68485.

The costs of publication of this article were defrayed in part by the payment of page charges. This article must therefore be hereby marked *advertisement* in accordance with 18 U.S.C. Section 1734 solely to indicate this fact.

We thank the Frances Williams Preston Laboratories of the TJ Martell Foundation for their generous support.

References

1. Cunha GR, Alarid ET, Turner T, Donjacour AA, Boutin EL, Foster BA. Normal and abnormal development of the male urogenital tract: role of androgens, mesenchymal-epithelial interactions, and growth factors. J Androl 1992;13:465–75.
2. Hayward SW, Haughney PC, Rosen MA, et al. Interactions between adult human prostatic epithelium and rat urogenital sinus mesenchyme in a tissue recombination model. Differentiation 1998;63:131–40.
3. Hayward SW, Cunha GR. The prostate: development and physiology. Radiol Clin North Am 2000;38:1–14.
4. Grossfeld G, Hayward S, Tlsty T, Cunha G. The role of stroma in prostatic carcinogenesis. Endocr Relat Cancer 1998;5:253–70.
5. Joesting MS, Perrin S, Elenbaas B, et al. Identification of SFRP1 as a candidate mediator of stromal-to-epithelial signaling in prostate cancer. Cancer Res 2005;65:10423–30.
6. Ao M, Franco OE, Park D, Raman D, Williams K, Hayward SW. Cross talk between paracrine-acting cytokine and chemokine pathways promotes malignancy in benign human prostatic epithelium. Cancer Res 2007; 67:4244–53.
7. Chung LW. Fibroblasts are critical determinants in prostatic cancer growth and dissemination. Cancer Metastasis Rev 1991;10:263–74.
8. Olumi AF, Grossfeld GD, Hayward SW, Carroll PR, Tlsty TD, Cunha GR. Carcinoma-associated fibroblasts direct tumor progression of initiated human prostatic epithelium. Cancer Res 1999;59:5002–11.
9. Ayala GE, Dai H, Tahir SA, et al. Stromal antiapoptotic paracrine loop in perineural invasion of prostatic carcinoma. Cancer Res 2006;66:5159–64.
10. Mueller MM, Fusenig NE. Friends or foes—bipolar effects of the tumour stroma in cancer. Nat Rev Cancer 2004;4:839–49.
11. Fu M, Wang C, Li Z, Sakamaki T, Pestell RG. Minireview: cyclin D1: normal and abnormal functions. Endocrinology 2004;145:5439–47.
12. Petty WJ, Dragnev KH, Dmitrovsky E. Cyclin D1 as a target for chemoprevention. Lung Cancer 2003;41 Suppl 1:S155–61.
13. Polsky D, Cordon-Cardo C. Oncogenes in melanoma. Oncogene 2003;22:3087–91.
14. Hunter T, Pines J. Cyclins and cancer. II: cyclin D and CDK inhibitors come of age. Cell 1994;79:573–82.
15. Sherr CJ. Mammalian G_1 cyclins. Cell 1993;73: 1059–65.
16. Bartkova J, Lukas J, Strauss M, Bartek J. Cyclin D1 oncoprotein aberrantly accumulates in malignancies of diverse histogenesis. Oncogene 1995;10:775–8.
17. Roy PG, Thompson AM. Cyclin D1 and breast cancer. Breast 2006;15:718–27.
18. Day KC, McCabe MT, Zhao X, et al. Rescue of embryonic epithelium reveals that the homozygous deletion of the retinoblastoma gene confers growth factor independence and immortality but does not influence epithelial differentiation or tissue morphogenesis. J Biol Chem 2002;277:44475–84.
19. Caldon CE, Daly RJ, Sutherland RL, Musgrove EA. Cell cycle control in breast cancer cells. J Cell Biochem 2006;97:261–74.
20. Arnold A, Papanikolaou A. Cyclin D1 in breast cancer pathogenesis. J Clin Oncol 2005;23:4215–24.
21. Chen Y, Martinez LA, LaCava M, Coghlan L, Conti CJ. Increased cell growth and tumorigenicity in human prostate LNCaP cells by overexpression to cyclin D1. Oncogene 1998;16:1913–20.
22. Pera M, Fernandez PL, Palacin A, et al. Expression of cyclin D1 and p53 and its correlation with proliferative activity in the spectrum of esophageal carcinomas induced after duodenal content reflux and 2,6-dimethylnitrosomorpholine administration in rats. Carcinogenesis 2001;22:271–7.
23. Hayward SW, Wang Y, Cao M, et al. Malignant transformation in a nontumorigenic human prostatic epithelial cell line. Cancer Res 2001;61:8135–42.
24. Hayward SW, Dahiya R, Cunha GR, Bartek J, Despande N, Narayan P. Establishment and characterization of an immortalized but non-tumorigenic human prostate epithelial cell line: BPH-1. In Vitro 1995;31A: 14–24.
25. Williams K, Fernandez S, Stien X, et al. Unopposed c-MYC expression in benign prostatic epithelium causes a cancer phenotype. Prostate 2005;63:369–84.
26. Hayward SW, Haughney PC, Lopes ES, Danielpour D, Cunha GR. The rat prostatic epithelial cell line NRP-152 can differentiate *in vivo* in response to its stromal environment. Prostate 1999;39:205–12.
27. Dalrymple S, Antony L, Xu Y, et al. Role of notch-1 and E-cadherin in the differential response to calcium in culturing normal versus malignant prostate cells. Cancer Res 2005;65:9269–79.
28. True L, Coleman I, Hawley S, et al. A molecular correlate to the Gleason grading system for prostate adenocarcinoma. Proc Natl Acad Sci U S A 2006;103: 10991–6.
29. Yasunaga Y, Nakamura K, Ewing CM, Isaacs WB, Hukku B, Rhim JS. A novel human cell culture model for the study of familial prostate cancer. Cancer Res 2001; 61:5969–73.
30. Barclay WW, Woodruff RD, Hall MC, Cramer SD. A system for studying epithelial-stromal interactions reveals distinct inductive abilities of stromal cells from benign prostatic hyperplasia and prostate cancer. Endocrinology 2005;146:13–8.
31. Seidman JD, Berman JJ, Moore GW, Yetter RA. Multiparameter DNA flow cytometry of keratoacanthoma. Anal Quant Cytol Histol 1992;14:113–9.
32. Tuxhorn JA, Ayala GE, Smith MJ, Smith VC, Dang TD, Rowley DR. Reactive stroma in human prostate cancer: induction of myofibroblast phenotype and extracellular matrix remodeling. Clin Cancer Res 2002;8:2912–23.
33. Bosman FT, de Bruine A, Flohil C, van der Wurff A, ten Kate J, Dinjens WW. Epithelial-stromal interactions in colon cancer. Int J Dev Biol 1993;37:203–11.
34. Seljelid R, Jozefowski S, Sveinbjornsson B. Tumor stroma. Anticancer Res 1999;19:4809–22.
35. De Cosse J, Gossens CL, Kuzma JF. Breast cancer: induction of differentiation by embryonic tissue. Science 1973;181:1057–8.
36. Fukamachi H, Mizuno T, Kim YS. Morphogenesis of human colon cancer cells with fetal rat mesenchymes in organ culture. Experientia 1986;42:312–5.
37. Singer C, Rasmussen A, Smith HS, Lippman ME, Lynch HT, Cullen KJ. Malignant breast epithelium selects for insulin-like growth factor II expression in breast stroma: evidence for paracrine function. Cancer Res 1995;55:2448–54.
38. Wright JH, McDonnell S, Portella G, Bowden GT, Balmain A, Matrisian LM. A switch from stromal to tumor cell expression of stromelysin-1 mRNA associated with the conversion of squamous to spindle carcinomas during mouse skin tumor progression. Mol Carcinog 1994;10:207–15.
39. Cunha GR, Ricke W, Thomson A, et al. Hormonal,

cellular, and molecular regulation of normal and neoplastic prostatic development. J Steroid Biochem Mol Biol 2004;92:221–36.
40. Hayward SW, Olumi AF, Haughney PC, Dahiya R, Cunha GR. Prostate adenocarcinoma causes dedifferentiation of its surrounding smooth muscle. Proc Am Urol Assoc 1996;155:605A.
41. Hayward SW, Rosen MA, Cunha GR. Stromal-epithelial interactions in normal and neoplastic prostate. Br J Urol 1997;79 Suppl 2:18–26.
42. Ellwood-Yen K, Graeber TG, Wongvipat J, et al. Myc-driven murine prostate cancer shares molecular features with human prostate tumors. Cancer Cell 2003;4:223–38.
43. Wang S, Gao J, Lei Q, et al. Prostate-specific deletion of the murine Pten tumor suppressor gene leads to metastatic prostate cancer. Cancer Cell 2003;4:209–21.
44. Hayward SW, Wang Y, Cao M, et al. Malignant transformation in a non-tumorigenic human prostatic epithelial cell line. Cancer Res 2001;61:8135–42.
45. Maffini MV, Soto AM, Calabro JM, Ucci AA, Sonnenschein C. The stroma as a crucial target in rat mammary gland carcinogenesis. J Cell Sci 2004;117:1495–502.
46. Pierce G. The benign cells of malignant tumors. In: King T, editor. Developmental aspects of carcinogenesis and immunity. New York: Academic Press, Inc.; 1974. p. 3–22.
47. Mintz B. Genetic mosaicism and *in vivo* analyses of neoplasia and differentiation. In: Saunders G, editor. Cell differentiation and neoplasia. New York: Raven Press; 1978. p. 27–56.
48. Hayashi N, Cunha GR. Mesenchyme-induced changes in neoplastic characteristics of the Dunning prostatic adenocarcinoma. Cancer Res 1991;51:4924–30.
49. Hayashi N, Cunha GR, Wong YC. Influence of male genital tract mesenchymes on differentiation of Dunning prostatic adenocarcinoma. Cancer Res 1990;50:4747–54.
50. Bhowmick NA, Chytil A, Plieth D, et al. TGF-β signaling in fibroblasts modulates the oncogenic potential of adjacent epithelia. Science 2004;303:848–51.
51. Weaver VM, Petersen OW, Wang F, et al. Reversion of the malignant phenotype of human breast cells in three-dimensional culture and *in vivo* by integrin blocking antibodies. J Cell Biol 1997;137:231–45.
52. Kallakury BV, Sheehan CE, Ambros RA, Fisher HA, Kaufman RP, Jr., Ross JS. The prognostic significance of p34cdc2 and cyclin D1 protein expression in prostate adenocarcinoma. Cancer 1997;80:753–63.
53. Bubendorf L, Kononen J, Koivisto P, et al. Survey of gene amplifications during prostate cancer progression by high-throughout fluorescence *in situ* hybridization on tissue microarrays. Cancer Res 1999;59:803–6.
54. Gumbiner LM, Gumerlock PH, Mack PC, et al. Overexpression of cyclin D1 is rare in human prostate carcinoma. Prostate 1999;38:40–5.
55. Han EK, Lim JT, Arber N, Rubin MA, Xing WQ, Weinstein IB. Cyclin D1 expression in human prostate carcinoma cell lines and primary tumors. Prostate 1998;35:95–101.
56. Givan AL. Cells from within: DNA in life and death. In: Flow Cytometry: First Principles (Second Edition). New York: Wiley-Liss, Inc.; 2001. p. 123–58.
57. Masuda A, Takahashi T. Chromosome instability in human lung cancers: possible underlying mechanisms and potential consequences in the pathogenesis. Oncogene 2002;21:6884–97.
58. Koivisto P. Aneuploidy and rapid cell proliferation in recurrent prostate cancers with androgen receptor gene amplification. Prostate Cancer Prostatic Dis 1997;1:21–5.

Tissue-Specific Consequences of Cyclin D1 Overexpression in Prostate Cancer Progression

Yue He, Omar E. Franco, Ming Jiang, et al.

Cancer Res 2007;67:8188-8197.